PHILOSOPHICAL MAGAZINE A, 1999, VOL. 79, NO. 1, 147–166

Study of the irradiation-induced $\alpha \rightarrow \omega$ phase transformation in titanium: kinetics and mechanism

By H. DAMMAK

Laboratoire Chimie Physique du Solide, Unité de Recherche associée au CNRS 453, Ecole Centrale Paris, Grande Voie des Vignes, 92295 Chatenay-Malabry, France

A. DUNLOP and D. LESUEUR†

Laboratoire des Solides Irradiés, Commissariat à l'Énergie Atomique–Ecole Polytechnique, 91128 Palaiseau Cedex, France

[*Received 1 May 1997 and accepted in revised form 13 March 1998*]

ABSTRACT

An atomic–crystallographic mechanism is proposed for the $\alpha \rightarrow \omega$ transformation during irradiation. The mechanism is based on the propagation of a localized displacement wave of the $[100]_\alpha$ close-packed rows. From the phonon dispersion curves along $(010)_\alpha$, the displacement wave is decomposed into two transverse optical phonons and one transverse acoustic phonon. The proposed mechanism accounts for the ω morphology and can explain the presence of $(2\bar{1}0)_\alpha$ planes of diffuse intensity in reciprocal space. The kinetic of the transformation was followed by *in-situ* length and electrical resistance measurements. An analytical model based on the proposed mechanism enabled us to fit the experimental curves. Finally the kinetic results were compared with those obtained previously for the transformation occurring under an applied static pressure.

§1. INTRODUCTION

Pure titanium (figure 1) exits in a hcp structure (α phase) at room temperature and pressure. It transforms to the bcc structure (β phase) at high temperatures (greater than 1155 K). At high pressures, titanium transforms to a simple hexagonal phase (ω phase). Many transformation pressures were reported in the literature (Sikka, 1982); they depend on experimental techniques and conditions. This is due to the existence of a wide hysteresis in the $\alpha \leftrightarrow \omega$ transformation leading to a retention of the high-pressure phase in a metastable state at room temperature and pressure (figure 1).

Recently we have shown that the $\alpha \rightarrow \omega$ transformation in titanium can also be obtained during irradiation at 20 K with 2.2 GeV uranium ions (Dammak *et al.* 1993).

When a gigaelectronvolt heavy ion (lead, tantalum, uranium, etc.) slows down in a material, it mainly loses its energy in electronic excitation and ionisation. The linear rate S_e of energy deposition in electronic processes (in kiloelectron volts per nanometre) can reach values as high as a few tens of kiloelectronvolts per nanometre and lead to a structural modification in titanium (Dammak *et al.* 1996). A study of

† Present address: DRECAM, Centre d'Etudes de Saclay, 91191 Gif-sur-Yvette, France.

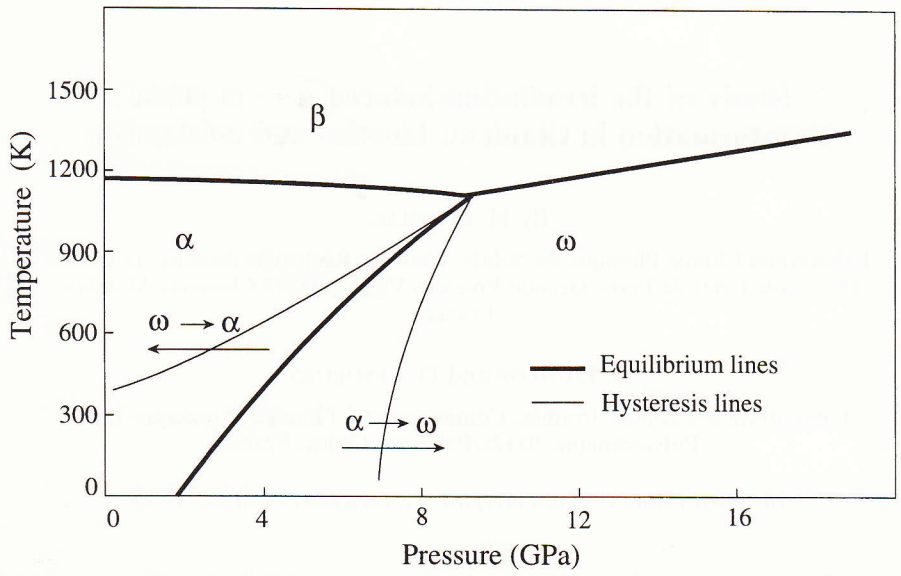

Figure 1. Temperature pressure phase diagram for titanium. The $\alpha \leftrightarrow \omega$ transformation under pressure is characterized by a wide hysteresis, leading to a retention of the ω phase in a metastable state at room temperature and pressure.

these structural modifications by transmission electron microscopy (TEM) after irradiation performed in various conditions (S_e, fluence and irradiation temperature) shows that the complete $\alpha \rightarrow \omega$ phase transformation is obtained after low-temperature (20–90 K) irradiation, for S_e higher than a threshold value S_e of about 33 keV nm^{-1} and for a fluence higher than 10^{12} ions cm^{-2}.

The available experimental results (phase change during irradiation) allowed us to settle the question of the mechanism by which *the transfer of deposited energy via electronic excitations to the lattice occurs* (Dammak *et al.* 1993). The suggested theoretical approach is based on the Coulomb explosion concept in which the electrostatic potential energy of the ionised atoms along the projectile wake is converted into kinetic energy (Lesueur and Dunlop 1993). It has been shown that collective and coherent motions of neighbouring atoms can generate a shock-wave. The response of a metal to such a shock wave depends on its elastic and mechanical properties and the created damage could consist of stable dislocation loops, stacking faults or point defects (Dammak *et al.* 1996). In the present paper we propose an atomic–crystallographic mechanism based on atomic motions leading to the $\alpha \rightarrow \omega$ phase change after the energy conversion.

In the following, we shall first present the known mechanisms for the $\alpha \rightarrow \beta$ and $\alpha \rightarrow \omega$ phase changes. Electron diffraction studies of gigaelectronvolt-ion-irradiated titanium show that the β phase is absent in the samples, so that a direct mechanism accounting for the $\alpha \rightarrow \omega$ phase change occurring during irradiation is proposed. It is shown in particular that three phonons are necessary to describe the corresponding displacement sequences.

In order to determine the kinetics of the evolution from the α to the ω phase, we present in the last section of the paper *in-situ* measurements during a low-temperature irradiation (performed in the GANIL accelerator in Caen (France)) of the electrical resistivity increase and the length change of a titanium ribbon. The

phase change leads not only to a high saturation resistivity increase ($\Delta\rho_\infty$ of a few tens of microhm centimetres (Dammak *et al.* 1993, 1996)) but also to a significant volume change because the ω phase is denser than the α phase. It is shown that the kinetics of the irradiation-induced phase change are very similar to that of the α → ω evolution observed in titanium submitted to a very high static pressure.

§2. Metastable ω phase characteristics

The hexagonal ω phase is described by the *P6/mmm* space group. The unit cell contains three atoms at two non-equivalent positions a and d: a, (0, 0, 0); d, $(\frac{1}{3}, \frac{2}{3}, \frac{1}{2})$, $(\frac{2}{3}, \frac{1}{3}, \frac{1}{2})$ (figure 2). The structure factor F_{hkl} has a zero intensity when $h - k \neq 3n$ and $l = 2n$[7]. The omega structure can be represented as piling of simple hexagonal planes A and honey hexagonal planes D. The density of D is twice that of A. If we consider the β phase (bcc) as a piling of hexagonal planes along $[111]_\beta$, that is ABCABC..., the D plane of ω structure is then obtained by collapsing B and C planes with A unchanged (figure 3(*b*)). This outline corresponds to the mechanism of the β → ω transformation obtained by quenching of some titanium alloys (Ti–V, Ti–Cr, etc.) (Silcock 1958, Sass 1972). The orientational relationships (ORs) between β and ω are

$$(111)_\beta \parallel (001)_\omega,$$

$$[0\bar{1}1]_\beta \parallel [100]_\omega.$$

As for the β → ω transformation, the mechanism of the α → β transformation is well established. First Burgers (1934) proposed a mechanism based on a shearing of $(001)_\alpha$ planes. Two neighbouring planes move in opposite direction along $[1\bar{1}0]_\alpha$ (figure 3(*a*)). This shearing is then followed by a contraction of 3% along $[110]_\alpha$ and by an expansion of 5.6% along $[1\bar{1}0]_\alpha$, thereby changing the angle from 120° to 109.5°. The ORs between α and β are

$$(002)_\alpha \parallel (01\bar{1})_\beta,$$

$$[100]_\alpha \parallel [111]_\beta.$$

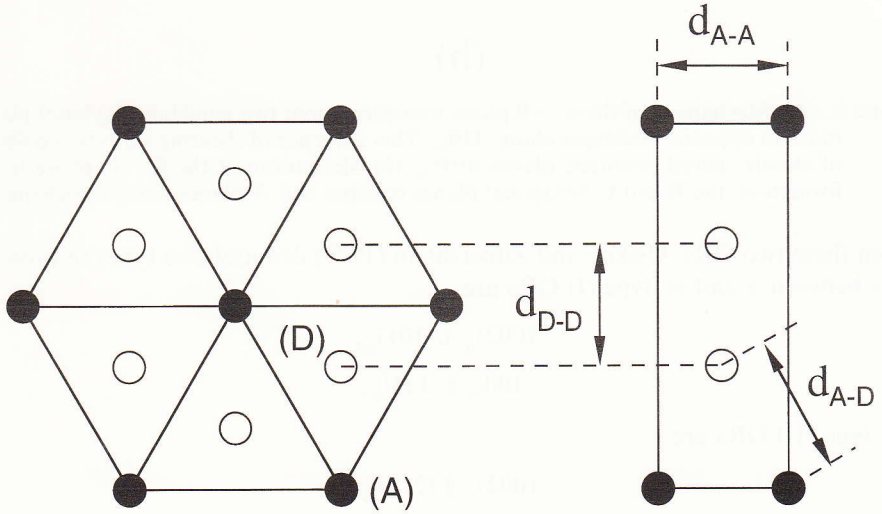

Figure 2. The hexagonal ω phase with two non-equivalent positions A and D.

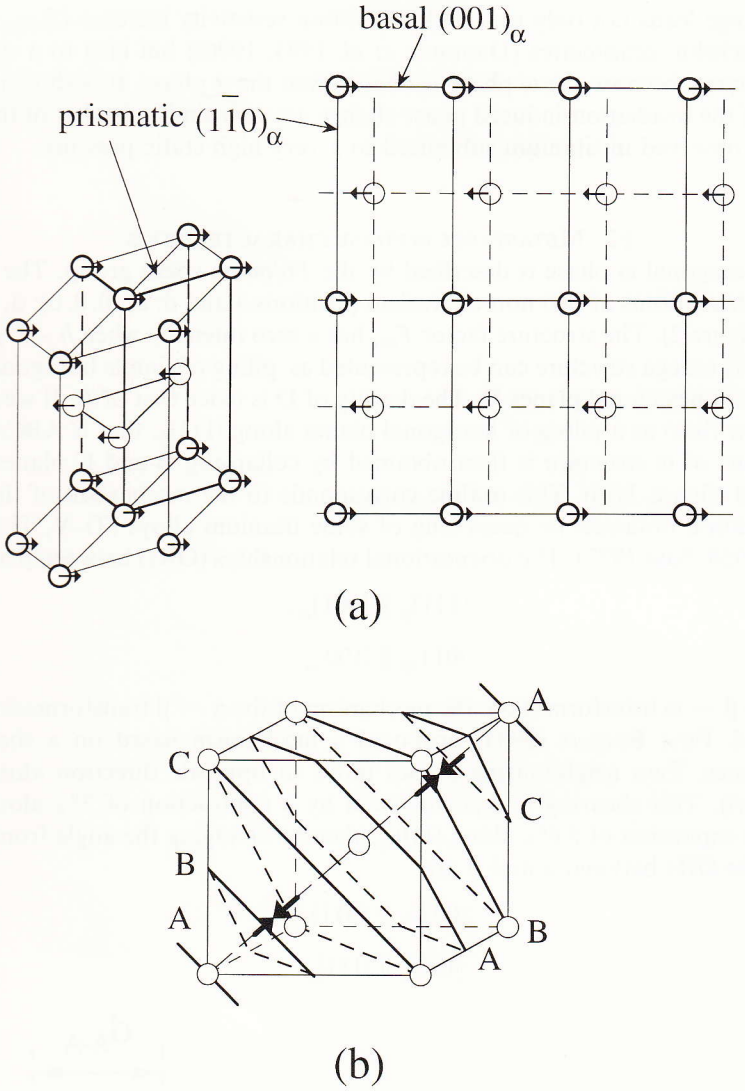

Figure 3. (*a*) Mechanism of the $\alpha \rightarrow \beta$ phase transformation: two neighbouring basal planes move in opposite directions along $[1\bar{1}0]_\alpha$. This sequence of shearing leads to a collapse of closely spaced prismatic planes $(010)_\alpha$. (*b*) Mechanism of the $\beta \rightarrow \omega$ phase transformation: the B and C hexagonal planes collapse and A planes remain unchanged.

From these two ORs, Usikov and Zilbershtein (1973) deduced two types of possible ORs between α and ω: type (I) ORs are

$$(002)_\alpha \parallel (101)_\omega,$$
$$[100]_\alpha \parallel [12\bar{1}]_\omega,$$

and type (II) ORs are

$$(002)_\alpha \parallel (2\bar{1}0)_\omega,$$
$$[100]_\alpha \parallel [001]_\omega,$$

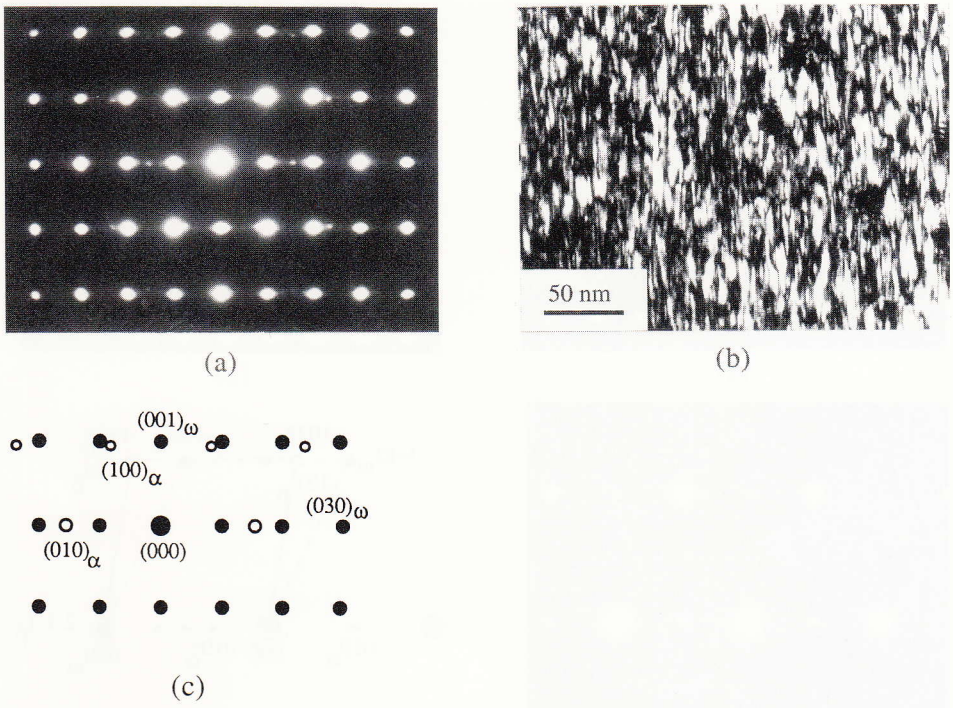

Figure 4. Titanium irradiated at 20 K with 2.2 GeV uranium ions at a fluence of 1.2×10^{13} ions cm^{-2}. (*a*) Electron diffraction pattern showing the $[100]_\omega$ and $[001]_\alpha$ Laue zones; (*b*) the dark-field image obtained using the $(001)_\omega$ spot showing that ω domains resemble laths lying in the α prismatic planes (i.e. perpendicular to $\mathbf{g} = (010)_\alpha$); (*c*) key to the pattern (*a*). The image (*b*) was first published (Dammak *et al.* 1993, figure 3 b1) with an inexact orientation; it was mistakenly rotated by 90°.

Song and Gray (1995) have shown a third type of OR, namely type (III) in shock-loaded zirconium:

$$(002)_\alpha \parallel (101)_\omega,$$

$$[210]_\alpha \parallel [111]_\omega.$$

Recently Jyoti *et al.* (1997) showed that ORs (I) and (III) are equivalent.

We note that for ORs (I) and (III) the close-packed planes $(002)_\alpha$ are parallel to the ω rugged planes $(101)_\omega$, whereas in OR (II) the close-packed planes of α and ω are parallel and also for close-packed rows.

In our case, only OR (II) was observed (figure 4). In the following section we present some properties observed on electron diffraction patterns and then discuss the mechanism of the α → ω transformation induced by the irradiation.

2.1. *Electron diffraction observations*

The dark-field image (figure 4(*b*)) shows the morphology of the projection of the ω phase domains. These domains resemble laths of 2 nm × 10 nm size lying in the prismatic planes $(010)_\alpha$. Figure 4(*a*)) shows the corresponding electron diffraction pattern on which α and ω reflections are indexed. Figure 5 shows different Laue zones obtained by tilting around $(010)_\alpha$ (i.e. $(030)_\omega$). One can easily observe diffuse

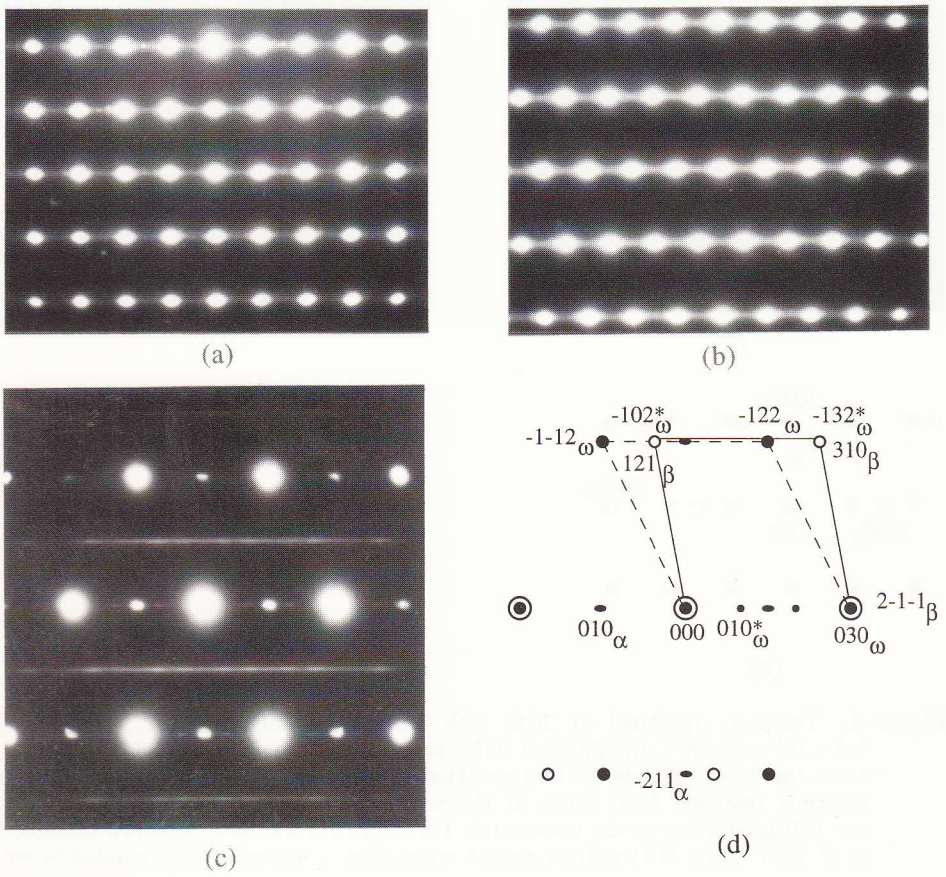

Figure 5. (*a*)–(*c*) Electron diffraction patterns obtained by tilting around $(030)_\omega$, showing (*a*) $[100]_\omega$, (*b*) $[10\bar{1}]_\omega$ and (*c*) $[201]_\omega$ Laue zones. (*d*) Key to the diffraction parttern (*c*) on which the $[1\bar{3}5]_\beta$ Laue zone is superposed according to the β–ω OR. The asterisks indicate that ω reflections are absent owing to systematic extinction.

intensity lines (streaks) parallel to the $(010)_\alpha$ direction in the reciprocal space. A close examination of streak directions indicates that the diffuse streaking can be described as sheets of intensity lying on $(001)_\omega(\| (2\bar{1}0)_\alpha)$ planes in reciprocal lattice. For example, if we consider the $[201]_\omega(\| [102]_\alpha)$ Laue zone (figure 5(*c*)), we observe lines which do not go through α or ω reflections. These lines come from intensity planes corresponding to $l = \pm 1$, $l = \pm 3$. On this diffraction pattern the lines coming from the planes $l = 0$; $l = \pm 2$ should pass through ω and α reflections. The intensity of such lines is very weak and could be explained by the systematic extinction in such planes. In fact, $l = 2p$ planes have two thirds of reflections absent, whereas $l = 2p + 1$ planes contain all possible reflections. In conclusion, there are $(001)_\omega$ and so $(2\bar{1}0)_\alpha$ planes of diffuse intensity in reciprocal lattice. The origin of the diffuse intensity is discussed below.

Concerning the existence of the β phase in the irradiated sample, if we consider the OR between β and ω and the systematic extinction in two structures, we note that $(h, k, l)_\beta$ reflections with $h + k + l = 4n'$ and $n' \neq 3n''$ coincide with the $(-h + 2k + 4n';\ 2h + k - 4n';\ 2n')_\omega$ reflections which are absent. For example, in

the Laue zone $[201]_\omega$, $(\bar{1}02)_\omega$ and $(\bar{1}32)_\omega$ which are absent may coincide with $(121)_\beta$ and $(310)_\beta$ respectively. Figure 5(*c*) shows that these β reflections are absent in this Laue zone, so that we can deduce the absence of the β phase.

ω cell parameters were determined by X-ray diffraction. We find that $a_\omega = 0.462$ nm and $c_\omega = 0.284$ nm. The ratio $\Omega = c_\omega/a_\omega$ was determined with more precision via the ratio G_{h00}/G_{00l} (modules of vectors in reciprocal space) measured directly in the $[100]_\omega$ Laue zones. We find that $c_\omega/a_\omega = 0.616 \pm 0.002$. This latter value is 0.6% greater than the ideal value $(\frac{3}{8})^{1/2} = 0.612$. We note that the experimental value of Ω coincides with the value which minimizes the differences between the different interatomic distances. In fact, in the ω cell we distinguish three nearest-neighbour spacings (figure 2):

$$d_{AA} = \Omega a_\omega,\ d_{DD} = \frac{1}{3^{1/2}} a_\omega,\ d_{AD} = (\tfrac{1}{3} + \tfrac{1}{4}\Omega^2)^{1/2} a_\omega.$$

For Ω between $1/3^{1/2}$ and $(\frac{2}{3})^{1/2}$, the distances are ordered as $d_{DD} < d_{AA} < d_{AD}$. The Ω value minimizing the differences between these distances obeys the equation

$$d_{AA} - d_{DD} = d_{AD} - d_{AA}$$

and is equal to $\Omega_0 = 16/(15 \times 3^{1/2}) = 0.6158$. On the other hand, a_α and c_α are approximately equal to c_ω and a_ω respectively. The c_ω/a_ω ratio approaches a_α/c_α which is close to 0.628.

2.2. *A transformation mechanism*

In the literature, two possible mechanisms were reported for the α → ω transformation: firstly an indirect mechanism and secondly a direct mechanism.

The indirect mechanism is based on the intermediate β phase: α → β → ω. This mechanism was proposed by Usikov and Zilberstein (1973) and Vohra *et al.* (1980).

Vohra *et al.* (1980) showed that a (ω + β) phase mixture is formed in Ti–10 at.% V alloy submitted to a high pressure (6.3 GPa) and that it should result from α → β and β → ω transformations.

A direct mechanism leading to the OR (II) was first proposed by Rabinkin *et al.* (1981) and then confirmed by Dobromyslov *et al.* (1990). The mechanism is based on short-range correlated displacements parallel to $[100]_\alpha$.

Song and Gray (1994) proposed a direct mechanism leading to the new OR (III). The lattice reconstruction during the transformation is divided into two parts: firstly a shearing in $(001)_\alpha$ planes and secondly a collapse of closely spaced $(010)_\alpha$ planes. These two parts are independent and one can obtain the transformation by applying the second part before the first part. However, the second part leads to an α → β transformation. Indeed, as shown in figure 3(*a*), the collapse of closely spaced prismatic planes corresponds to the Burgers mechanism for the α → β transformation. On the other hand, as mentioned by Jyoti *et al.* (1997), the OR (III) is equivalent to (I) for which Usikov and Zilbershtein (1973) have proposed the indirect mechanism. The proposed mechanism leading to the OR (III) is therefore an indirect mechanism based on the intermediate β phase.

In our case, for the α → ω transformation during irradiation, only the OR (II) was observed. We thus try to use the direct mechanism proposed by Rabinkin *et al.* (1981) in order to explain the defect structure observed in the retained ω phase.

If three neighbouring close-packed atomic rows $[100]_\alpha$ are displaced in the basal plane $(001)_\alpha$ on a small distance $a_\alpha/4$ along the $[100]_\alpha$ direction and if the next three

parallel atomic rows are displaced on the same distance along the opposite direction $[\bar{1}00]_\alpha$ and so on, the ω structure is formed according to the second orientational relationship (i.e. $(100)_\alpha \parallel (\bar{2}10)_\omega$ and $[100]_\alpha \parallel [001]_\omega$). Then additional small atomic shuffles of the order of $3^{1/2}a_\alpha/24$ are needed in directions close to $[120]_\alpha$ to obtain non-distorted $(001)_\omega$ hexagonal planes (figure 6).

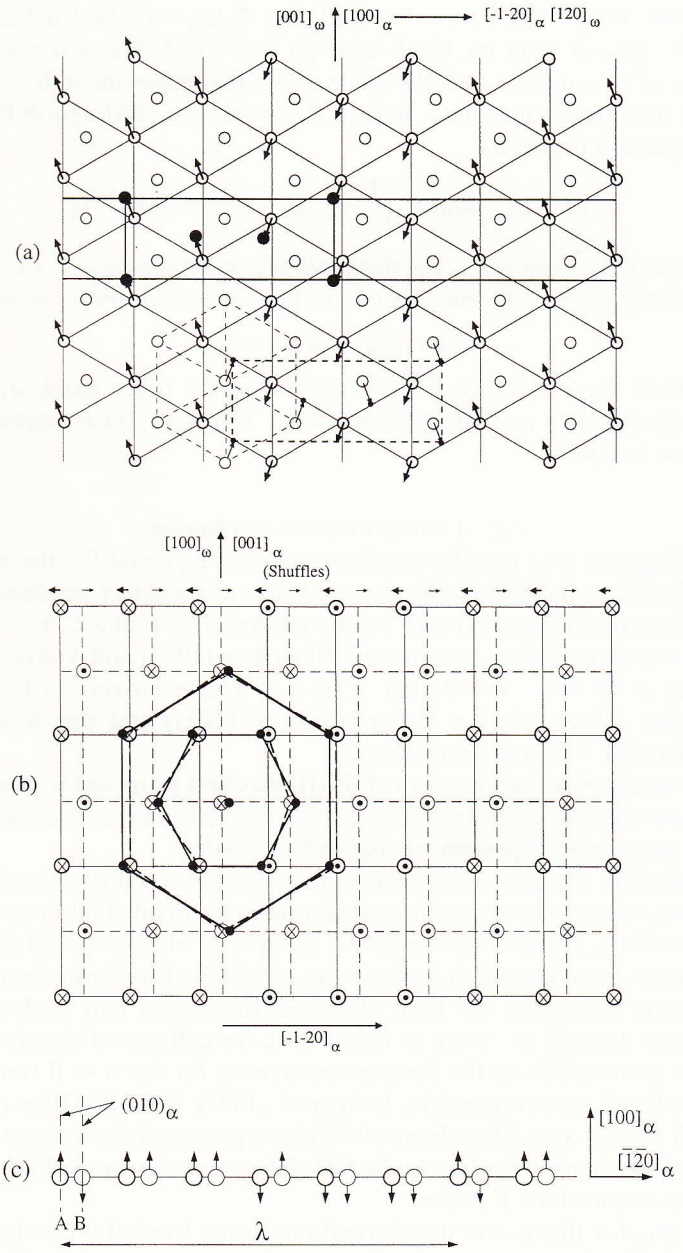

Figure 6. Mechanism of the $\alpha \rightarrow \omega$ phase transformation: (*a*) displacement of $[100]_\alpha$ close-packed atomic rows in the basal plane. (*b*) shuffles in order to obtain the non-distorted $(001)_\omega$ hexagonal plane; (*c*) schema of the transverse wave along $[120]_\alpha$ with a period of $\lambda = 3^{3/2}a_\alpha$. A and B are two closely spaced prismaic planes.

Considering the essential displacement close to $[100]_\alpha$ and neglecting the shuffles, the mechanism corresponds to transverse displacements along $[100]_\alpha$ of $(010)_\alpha$ prismatic planes. One can describe the hcp sequence in the $[120]_\alpha(\perp(010)_\alpha)$ direction as ABAB..., where the A–A separation is equal to $3^{1/2}a_\alpha/2$ (figure 6(*c*)). The displacements of planes is periodic with $\lambda = 6 \times 3^{1/2}a_\alpha/2$ (12 planes) and can be described by phonons of parallel transverse acoustic ($TA_\parallel$) and parallel transverse optic ($TO_\parallel$) branches in the $(010)_\alpha$ direction in the reciprocal lattice. In fact, after a simple Fourier decomposition (appendix A) the transverse displacement is expressed as following for A and B planes respectively:

$$u_n^A = \frac{a_\alpha}{4}\left[\frac{4}{3}\cos\left(n\frac{\pi}{3}\right) - \frac{1}{3}(-1)^n\right],$$

$$u_n^B = \frac{a_\alpha}{4}\left[-\frac{4}{3}\cos\left(n\frac{\pi}{3}+\frac{2\pi}{3}\right) + \frac{1}{3}(-1)^n\right].$$

The transverse displacement wave is clearly composed of one acoustic phonon with $q_1 = \frac{1}{6}(010)_\alpha$ and two optical phonons with $q_1 = \frac{1}{6}(010)_\alpha$ and $q_3 = \frac{1}{2}(010)_\alpha$ (figure 7).

If these three phonons act simultaneously, large defect-free ω domains are obtained. However, experimental results usually show that the ω phase contains many defects (stacking fault, dislocations, etc.).

A fine microstructure is also present in the ω phase obtained by irradiation, so that one can deduce that these phonons do not simultaneously act during the α → β transformation under irradiation.

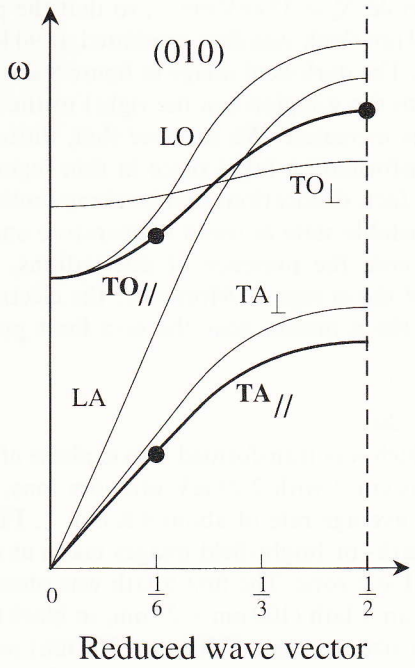

Figure 7. Titanium phonon spectrum in the $(010)_\alpha$ ($TA_\parallel$ and $TO_\parallel$ branches are represented by bold curves, after Stassis *et al.* (1979)): (●), three phonons responsible for the α → ω-phase transformation.

The $TO_{\parallel}\frac{1}{2}(010)_{\alpha}$ mode corresponds to a shearing of neighbouring AA or BB planes. As was shown by Tyson (1967) and Legrand (1984), the deformation by slip in hcp metals occurs almost entirely in the $\langle 100\rangle_{\alpha}$ close-packed directions. In titanium the primary slip plane (i.e. the most energetically favourable) is the prismatic plane. Dobromyslov *et al.* (1998) show that under 8 GPa static pressure, the $\alpha \rightarrow \omega$ phase transformation does not occur at room temperature in Zr–(40–95) at.% Ti alloys. The TEM observations show a dense dislocation structure in the α matrix. This supports the present direct mechanism of $\alpha \rightarrow \omega$ transition.

As mentioned previously (Dammak *et al.* 1996), during the irradiation each incoming ion creates a track along its path. The track is characterized by an alignment of a small damaged zones resembling dislocation loops of 3–5 nm size. With the phonon description, we propose that each dislocation loop results from a localized $TO_{\parallel}\frac{1}{2}(010)_{\alpha}$ phonon. When these damaged zones begin to overlap spatially, that is when the ion fluence is increased (greater than $5 \times 10^{12}\,\mathrm{cm}^{-2}$), the created loops are piled up. To minimize the stress energy, a local atomic rearrangement takes place, leading to the formation of ω domains. This rearrangement should to be the result of the action of $TO_{\parallel}$ and $TA_{\parallel}$ phonon modes, with $q_1 = \frac{1}{6}(010)_{\alpha}$. During the overlaps, stacking faults and dislocation loops are piled up randomly, so that the probability to build the correct sequence of displacements is very weak. This might explain the small size of ω laths close to $[120]_{\alpha}$ direction ($\parallel [120]_{\omega}$). This mechanism is confirmed by the two following results.

2.2.1. *Surface relaxation*

We observe the phase transformation in titanium irradiated by 0.9 GeV tantalum ions up to a fluence of 5.7×10^{13} ions cm^{-2}. The linear rate of energy deposition by such ions lies at the threshold $S_e^t \approx 33\,\mathrm{keV\,nm}^{-1}$, so that the phase change can take place. Titanium ribbon 14 μm thick was first irradiated at 90 K and then electrochemically thinned at −30°C. The dark-field image in figure 8 shows the limit between α and ω regions. Going from the α region (on the right) to the ω region (on the left), the thickness of the foil is increased. We suppose that, during the electrochemical polishing, the $\omega \rightarrow \alpha$ transformation takes place in thin regions caused by a strain relaxation on surfaces. In fact, dislocations and stacking faults are necessary for the ω phase to exist in a metastable state at room temperature and pressure conditions. In this image we easily note the presence of dislocations, the density of which increases in the vicinity of the ω region. Moreover, the electron diffraction pattern shows a mosaic form of the α matrix near the ω–α limit probably caused by the strong strain gradient.

2.2.2. *Annealing of the ω phase*

A titanium sample, which was transformed into ω phase after 20 K irradiation at a fluence of 1.2×10^{13} ions cm^{-2} with 2.2 GeV uranium ions, was gradually heated from 300 to 1060 K at an average rate of about $4\,\mathrm{K\,min}^{-1}$. Figure 9 shows electron diffraction patterns and dark- or bright-field images taken at different temperatures using the $[100]_{\omega}(\parallel [001]_{\alpha})$ Laue zone. The first α lath was observed between 520 and 570 K. Figure 9 (*b*) shows an α lath (100 nm × 25 nm, in black). Figure 9 (*c*) taken at 610 K shows that the lath size increases (370 nm × 100 nm) as the temperature gets higher. Above 610 K the ω phase was completely annealed and the restored α matrix contained a very complex dislocation structure which continued to be annealed at 1060 K (figures 9 (*d*)–(*f*)). This annealing experience shows two important points:

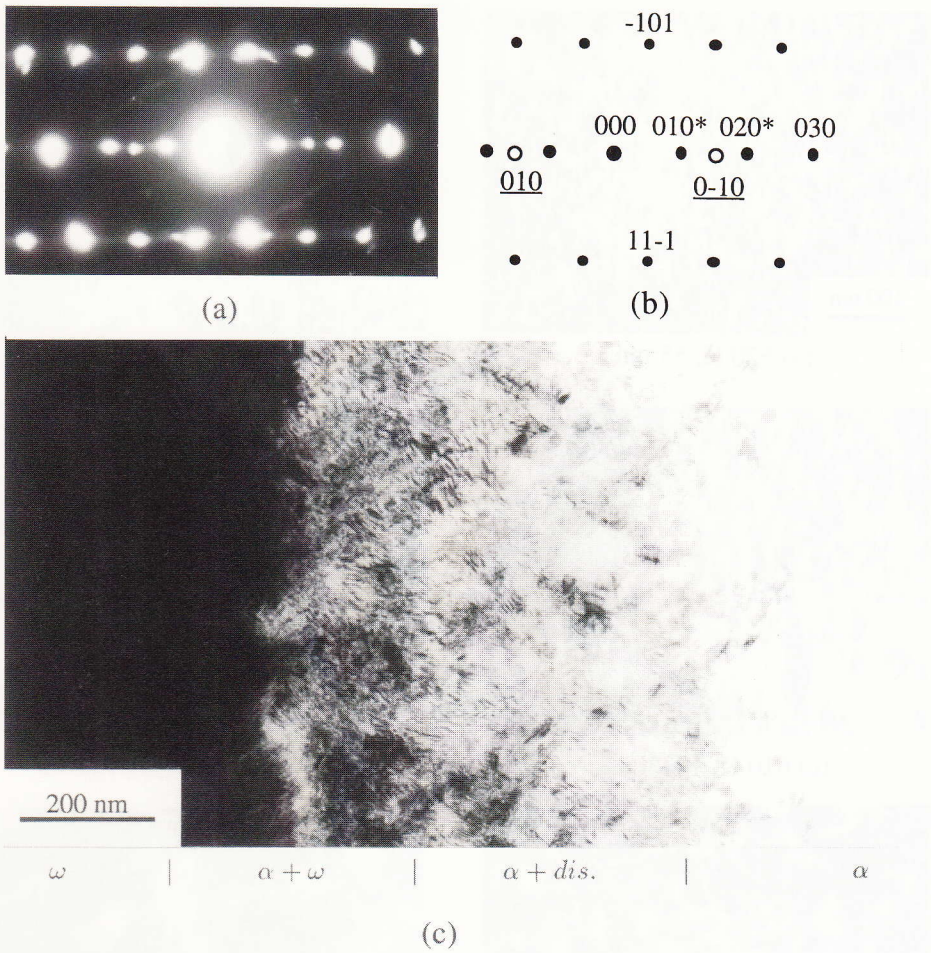

Figure 8. Titanium irradiated at 90 K with 0.9 GeV tantalum ions at a fluence of 5.7×10^{13} ions cm^{-2}: (*a*) diffraction pattern shows $[101]_\omega$ and almost $[101]_\alpha$ Laue zones, (*b*) key to the diffraction pattern, where α spots are represented by open circles; (*c*) dark-field image obtained using the $(010)_\alpha$ spot showing the frontier between α and ω regions (dis. means dislocations).

firstly the remaining α phase contains dislocations and secondly, when α laths appear, they lie in the primatic planes.

The α → ω phase transformation should obey the direct mechanism based on localized displacement waves of $\langle 100 \rangle_\alpha$ close-packed atomic rows in the α phase.

In the following the kinetics of the evolution from α to ω during irradiation are determined by measuring *in situ* the length change of a pure titanium ribbon.

§3. Kinetic experimental results

A polycrystalline titanium ribbon (20 mm × 1.8 mm × 14 μm) was irradiated at 20 K with 2.4 GeV uranium ions in a helium atmosphere. The average rate of linear energy deposition of the projectiles in the target is equal to 39.5 keV nm^{-1}. During the irradiation we measure *in situ* the evolution of the electrical resistance and of the length (Dunlop *et al.* 1989) of the ribbon as a function of the ion fluence Φ.

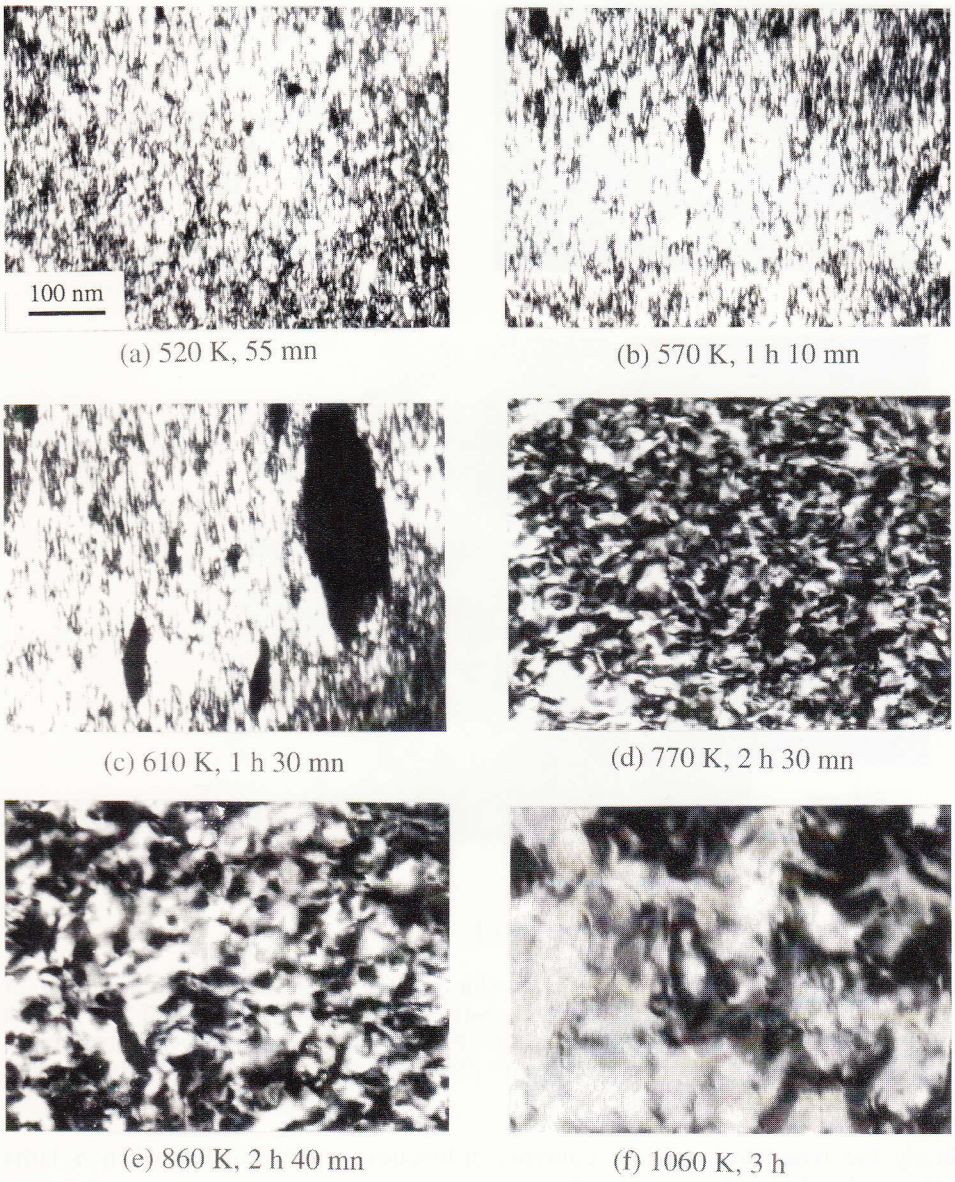

Figure 9. TEM observations during the annealing of the ω phase, where the titanium sample was irradiated at 20 K by 2.2 GeV uranium ions at a fluence of 1.2×10^{13} ions cm^{-2}: (*a*)–(*c*) dark-field images obtained using $(001)_\omega$ spot in the $[100]_\omega$ Laue zone (see figures 4 (*a*) and (*c*)); (*d*)–(*f*) bright-field images showing the annealing of dislocations.

Figure 10 shows that the length L of the ribbon increases at low fluences (stage I) with an initial growth rate $\dot{\delta}_0 = [\mathrm{d}(\Delta L/L_0)/\mathrm{d}\Phi]_{\Phi=0} = (\mathrm{d}\delta/\mathrm{d}\Phi)_{\Phi=0}$ equal to 2×10^{-17} cm^2 ion^{-1} and that the maximum length increase $\Delta L/L_0 \approx 0.02\%$ is reached at a fluence of 7×10^{11} ions cm^{-2}. Then the sample length contracts continuously (stage H) until the end of irradiation ($\delta \approx -0.17\%$ at a fluence of 6×10^{12} ions cm^{-2}. On the other hand the electrical resistance continuously increases during irradiation. We shall see below that the form factor of the sample stays

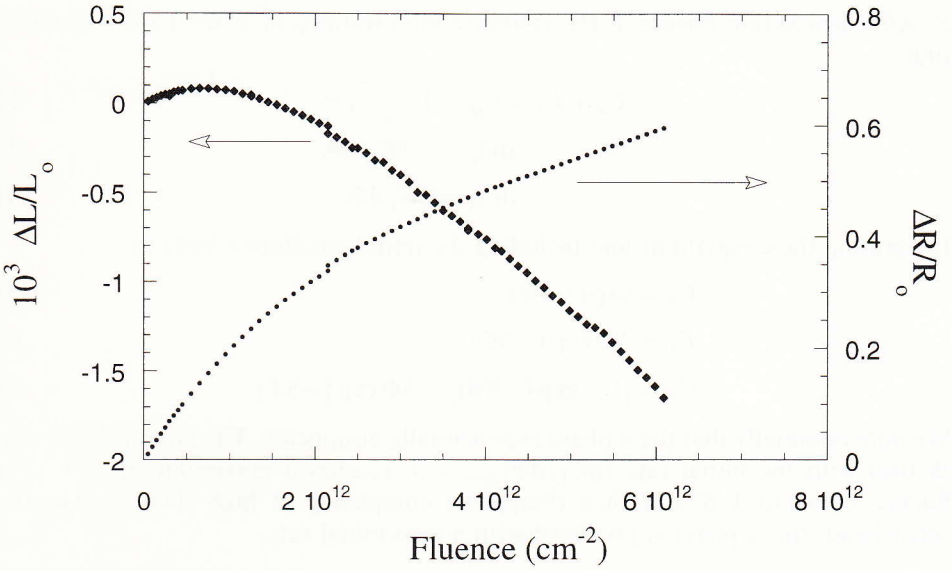

Figure 10. Relative length change and relative electrical resistance increase of a titanium ribbon during irradiation at 20 K by 2.4 GeV uranium ions.

almost unchanged, so that the results can easily be converted into electrical resistivity changes, leading to an initial rate of variation in the resistivity $\Delta\dot{\rho}_0 = [\mathrm{d}(\Delta\rho)/\mathrm{d}\Phi]_{\Phi=0}$ equal to $5 \times 10^{-12}\ \mu\Omega\,\mathrm{cm}^3$.

§4. Kinetic model

As shown above, the contraction of the length should to be a result of the $\alpha \rightarrow \omega$ phase transformation. The initial length increase cannot be explained by the phase change. At low fluences each incident ion creates a track along its path; the track is characterized by an alignment of a small damaged zones resembling dislocation loops of about 3 nm diameter. Around the dislocation lines, atoms shift from their periodic positions in the hcp arrangement leading to a local volume expansion. During stage I of irradiation, the creation of damage inside the tracks leads to a swelling, that is macroscopic volume (and thus length) increase.

Increasing the ion fluence (stage H), the tracks begin to overlap, the created loops are piled up and a local atomic rearrangement takes place to minimize the stress energy leading to the formation of ω domains.

To describe quantitatively the phase change during irradiation the following model is proposed. The phase transition is decomposed into two states:

$$\alpha \rightarrow \Delta \rightarrow \omega. \tag{1}$$

The intermediate Δ state is the α phase with microstructural modifications (i.e. the small damaged zones in the track). One incoming ion creates these defective zones. If a newly created defective region overlaps with a pre-existing Δ zone, ω phase is formed. The volume concentrations of α, Δ and ω states are denoted C_α, C_1 and C_ω respectively. The cross-section for the creation of Δ or ω is denoted

S. After irradiation fluence Φ the volume concentrations obey the following equations:

$$C_\alpha + C_1 + C_\omega = 1, \tag{2}$$

$$dC_\alpha = -SC_\alpha \, d\Phi, \tag{3}$$

$$dC_\omega = SC_1 \, d\Phi. \tag{4}$$

Integrating these equations and including the initial conditions leads to

$$C_\alpha = \exp(-S\Phi), \tag{5}$$

$$C_1 = S\Phi \exp(-S\Phi), \tag{6}$$

$$C_\omega = [1 - \exp(-S\Phi)] - S\Phi \exp(-S\Phi). \tag{7}$$

We note essentially that the α phase exponentially disappears. The intermediate state Δ rises with the initial rate $(dC_1/d\Phi)_{\Phi=0} = S$, reaches a maximum fraction at a fluence equal to $1/S$ and then disappears completely at high fluences. On the other hand, the ω phase is produced with a zero initial rate.

4.1. *Relative variation in the ribbon length*

After a fluence Φ, the Δ and ω zones induce a growth $\delta_1 C_1$ and a contraction $\delta_\omega C_\omega$ respectively of the sample. The relative length change of the ribbon is deduced in a linear hypothesis

$$\delta = \delta_1 C_1 - \delta_\omega C_\omega. \tag{8}$$

Using equations (6)–(8), the fit of the experimental curve (figure 11) gives

$$S = (2.3 \pm 0.3) \times 10^{-13} \text{ cm}^2,$$

$$\delta_1 = 0.89 \times 10^{-3},$$

$$\delta_\omega = 4.59 \times 10^{-3}.$$

δ_ω is coherent with the awaited value, as the corresponding atomic volume variation (about $3\delta_\omega$) is close to the value found in the literature: 1.3×10^{-2} (Sikka *et al.* 1982).

δ_1 is a fifth of δ_ω, which is a correct value corresponding to a swelling induced by dislocation loops. This value will be related in the following to the cross-section of defect damage creation.

4.2. *Electrical resistivity increase*

The electrical resistance R is related to the electrical resistivity ρ by the shape factor L/s, where L and s are length and the cross-section respectively of the ribbon:

$$R = \rho \frac{L}{s},$$

$$\frac{\Delta R}{R_0} = \frac{\Delta L}{L_0} - \frac{\Delta s}{s_0} + \frac{\Delta \rho}{\rho_0} \approx -\frac{\Delta L}{L_0} + \frac{\Delta \rho}{\rho_0},$$

with $r = \Delta\rho/\rho_0$

$$\frac{\Delta R}{R_0} = -\delta + r. \tag{9}$$

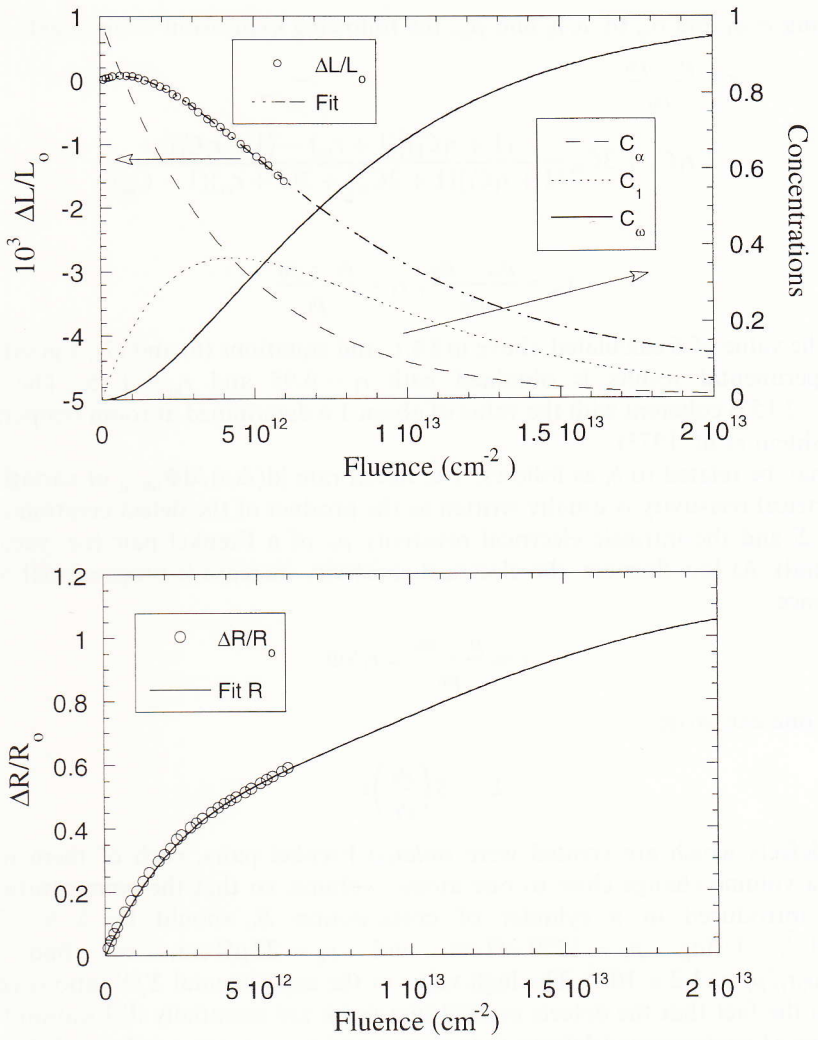

Figure 11. Fit of experimental kinetic results by the model proposed for the α → ω phase transformation.

According to experimental results, $\Delta R/R_0$ is two order of magnitudes higher than δ, so that $r = \Delta R/R_0$.

In order to calculate the resultant electrical resistivity during irradiation, one has to use an inhomogenous model considering spherical ω inclusions (with an electrical conductivity σ_ω) distributed in an α matrix, the resistivity of which varies during the irradiation owing to the presence of a concentration C_1 of dislocation loops. The resistivity of the α matrix, in a homogeneous model is $\rho_1 = \rho_0(1 + r_1 C_1)$, where ρ_0 is the electrical resistivity of the sample before irradiation and $r_1 C_1$ the relative resistivity variation due to the presence of dislocation loops.

The electrical conductivity σ of the intimate mixture of α and ω phases is given by (Landauer 1952)

$$\frac{\sigma - \sigma_1}{\sigma + 2\sigma_1} = C_\omega \frac{\sigma_\omega - \sigma_1}{\sigma_\omega + 2\sigma_1}. \tag{10}$$

Replacing σ, σ_1 and σ_ω by ρ, ρ_1 and ρ_ω, the following expression is obtained:

$$r = \frac{\rho - \rho_0}{\rho_0}$$

$$= r_1 C_1 + 3C_\omega \frac{(1 + r_1 C_1)[(1 + r_\omega) - (1 + r_1 C_1)]}{(1 + r_1 C_1)(1 + 2C_\omega) + 2(1 + r_\omega)(1 - C_\omega)}, \tag{11}$$

with

$$r_\omega = \frac{\rho_\omega - \rho_0}{\rho_0}, \quad r_1 = \frac{\rho_1 - \rho_0}{\rho_1}.$$

Using the value of S calculated above in § 4.1, and equations (6) and (7), a good fit of the experimental results is obtained with $r_1 = 0.95$ and $r_\omega = 1.15$. The ratio $\rho_\omega/\rho_0 = 2.15$ is coherent with the value of about 1.6 determined at room temperature (Zilbershtein *et al.* 1973).

r_1 may be related to δ_1 as follows. The initial rate $[\mathrm{d}(\Delta\rho)/\mathrm{d}\Phi]_{\Phi=0}$ of variation in the electrical resistivity is usually written as the product of the defect creation cross-section Σ and the intrinsic electrical resistivity ρ_F of a Frenkel pair (i.e. vacancy–interstitial). At low fluences, the electrical resistivity increase is proportional to the ion fluence:

$$r = \frac{\rho - \rho_0}{\rho_0} = r_1 S \Phi, \tag{12}$$

so that one can write

$$\Sigma = S\left(\frac{\rho_0}{\rho_F}\right) r_1. \tag{13}$$

If the defects which are created were *isolated* Frenkel pairs, each of them would induce a volume change close to one atomic volume, so that the concentration of defects introduced in a cylinder of cross-section S, should be $\Sigma/S = 3\delta_1 \approx 2.7 \times 10^{-3}$. Using $\rho_F = 1750\ \mu\Omega\,\mathrm{cm}$ and $\rho_0 = 22\ \mu\Omega\,\mathrm{cm}$, we find that $\Sigma/S = \rho_0 r_1/\rho_F \approx 1.2 \times 10^{-2}$. The high value of the experimental Σ/S ratio is coherent with the fact that the defects created in a track are essentially dislocation loops consisting of *agglomerated* defects; they correspond to an average volume change per defect much lower than that of isolated defects.

The kinetics of the phase transformation under an applied static pressure were studied by Singh *et al.* (1983). The fraction $\zeta(t)$ of formed ω phase as a function of time is determined from electrical resistance measurements as we did in an inhomogenous model (i.e. spherical ω inclusions with a conductivity σ_ω distributed in an α matrix with a conductivity $\sigma_\alpha = \sigma_0$). However, Singh *et al.* showed that $\zeta(t)$ curves could be fitted by the Avrami (1939) model

$$\zeta(t) = 1 - \exp\left[-\left(\frac{t}{\tau}\right)^n\right], \tag{14}$$

where the relaxation time τ and the power n depend ion the applied pressure. n is greater than unity and τ decreases rapidly when the pressure increases. From $n > 1$, we deduce that the initial ω-phase production rate is equal to zero so that, under a static pressure, the α phase does not transform directly into the ω phase. Singh *et al.* deduced that the ω phase appears after an incubation time. In our case an incubation fluence can be defined as the intersection of the tangent at the inflection point of the

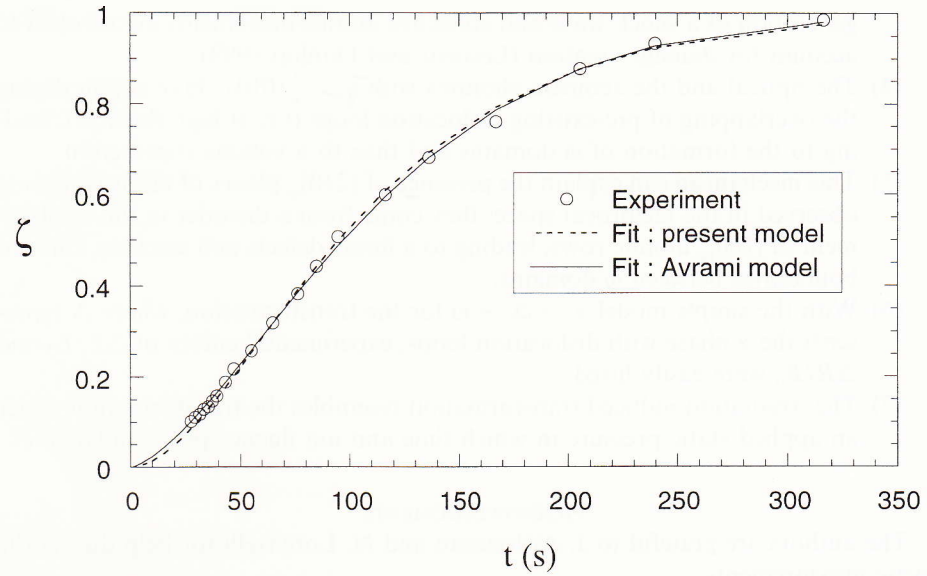

Figure 12. Experimental results obtained by Singh *et al.* (1983) for the transformation under an applied static pressure. The fraction $\zeta(t)$ of ω phase is fitted by the Avrami model $1 - \exp[-(t/\tau)^n]$ which depends on two parameters and by our model $[1 - \exp(-t/\tau)] - (t/\tau)\exp(-t/\tau)$ which depends on one parameter.

$C_\omega(\Phi)$ curve with the fluence axis. It is found to be of the order of 1.2×10^{12} ions cm^{-2}.

Figure 12 shows a good fit of $\zeta(t)$ experimental curve with the present model (equation (7)). The kinetics of the transformation seem to be the same under irradiation or under an applied static pressure.

§ 5. Conclusions

A detailed study of the α → ω phase transformation during and after irradiation allows us to propose a mechanism for the rearrangement of the lattice.

(1) The mechanism is based on propagation of a localized displacement wave of $[100]_\alpha$ close-packed rows as proposed by Rabinkin *et al.* (1981) and Dobromyslov *et al.* (1990).

(2) In the $TO_\parallel$ and $TA_\parallel$ branches of phonon spectrum along $(010)_\alpha$, three phonons are necessary to describe the transverse displacement wave: two optical phonons with $q_1 = \frac{1}{6}(010)_\alpha$ and $q_3 = \frac{1}{2}(010)_\alpha$ and one acoustic phonon with $q_1 = \frac{1}{6}(010)_\alpha$.

(3) The $TO_\parallel$ phonon with $q_3 = \frac{1}{2}(010)_\alpha$ which corresponds to a shearing of α prismatic planes along $[100]_\alpha$ seems to take action at low fluences in the formation of dislocation loops in an ion track and thus to a volume expansion of the α matrix (the formation of a state called Δ). The formation of dislocation loops is a result of the high-energy deposition in electronic processes which occurs as the ions slow down in the material (Dammak *et al.* 1996). The conversion of the deposited energy into atomic motion was previously explained by using the Coulomb explosion concept in which the

generation of a shock wave and collective atomic movements are invoked to account for damage creation (Lesueur and Dunlop 1993).

(4) The optical and the acoustic phonons with $q_1 = \frac{1}{6}(010)_\alpha$ take action during the overlapping of pre-existing dislocation loops (i.e. at high fluences), leading to the formation of ω domains and thus to a volume contraction.

(5) This mechanism can explain the presence of $(2\bar{1}0)_\alpha$ planes of diffuse intensity observed in the reciprocal space; they come from a disorder in the displacement of $[100]_\alpha$ atomic rows, leading to a linear defects and stacking faults at boundaries between ω domains.

(6) With the simple model $\alpha \rightarrow \Delta \rightarrow \omega$ for the transformation, where Δ represents the α phase with dislocation loops, experimental curves of $\Delta L/L_0$ and $\Delta R/R_0$ were easily fitted.

(7) The irradiation-induced transformation resembles the transformation under an applied static pressure in which time and ion fluence play similar roles.

Acknowledgments

The authors are grateful to J. Ardonceau and N. Lorenzelli for help during the kinetic measurements.

APPENDIX

We try to find the phonons responsible for the $\alpha \rightarrow \omega$ phase transformation. The hcp sequence of prismatic planes in the $[120]_\alpha$ direction can be described as ABAB..., where the A–A or B–B separation is equal to $a = (3^{1/2}/2)a_\alpha$. As mentioned above the ω phase is obtained by transverse displacements parallel to $[100]_\alpha$ of prismatic planes (figure 6(*c*)). Let u_n and v_n be the transverse displacements from the equilibrium positions of planes A and B respectively. From this sequence we have to consider differently the A–A, A–B and B–A interactions, which are separated by a, $b = a/3$ and $a - b = 2a/3$ respectively. Let α, β and γ be the corresponding massive force constants in an harmonic approximation.

To solve the equations of motion we seek solutions of the form:

$$\begin{aligned} u_n &= U \exp(\mathrm{i}qna - \mathrm{i}\omega t), \\ v_n &= V \exp(\mathrm{i}qna - \mathrm{i}\omega t). \end{aligned} \tag{A 1}$$

We find that

$$\omega^2 = 4\alpha \sin^2\left(\frac{qa}{2}\right) + (\beta + \gamma)\left\{1 \pm \left[1 - \frac{4\beta\gamma}{(\beta+\gamma)^2}\sin^2\left(\frac{qa}{2}\right)\right]^{1/2}\right\} \tag{A 2}$$

and

$$U = \pm \exp(-\mathrm{i}\theta_q)\, V, \tag{A 3}$$

with

$$\tan(\theta_q) = \frac{\gamma \sin(qa)}{\beta + \gamma\cos(qa)}. \tag{A 4}$$

The + and − signs correspond to acoustic and optic modes respectively.

Consider now the following schema of displacements (U_n, V_n) for the phase transformation:

$$\begin{aligned} &U_{-2} = -1, U_{-1} = 1, U_0 = 1, U_1 = 1, U_2 = -1, U_3 = -1, \\ &V_{-2} = -1, V_{-1} = -1, V_0 = 1, V_1 = 1, V_2 = 1, V_3 = -1, \\ &U_{n+6} = U_n, V_{n+6} = V_n. \end{aligned} \tag{A 5}$$

We decompose these displacements in the basis of normal modes as

$$\begin{pmatrix} U_n \\ V_n \end{pmatrix} = \sum_q A_q \begin{pmatrix} 1 \\ \exp(\mathrm{i}\theta_q) \end{pmatrix} \exp(\mathrm{i}qna) + B_q \begin{pmatrix} 1 \\ -\exp(\mathrm{i}\theta_q) \end{pmatrix} \exp(\mathrm{i}qna) \tag{A 6}$$

with $A_{-q} = A_q^*$ and $B_{-q} = B_q^*$. Taking the periodicity of $6a$ into account, the possible wave-vectors are $q_1 = (\pi)/(3a)$, $q_2 = (2\pi)/(3a)$, $q_3 = (\pi/a)$ and their opposites. From equation (A 5) we note that $V_n = U_{n-1}$, so that equation (A ,6) becomes

$$\begin{aligned} &U_n = \sum_q C_q \exp(\mathrm{i}qna), \\ &A_q - B_q = C_q \exp(-\mathrm{i}qa - \mathrm{i}\theta_q), \\ &C_q = A_q + B_q. \end{aligned} \tag{A 7}$$

After resolution of these equations for $n = -2$ to 3 we easily find that

$$\begin{aligned} A_1 &= \frac{1}{3}\left[1 + \exp\left(\frac{-\mathrm{i}\pi}{3} - \mathrm{i}\theta_1\right)\right], A_2 = 0, A_3 = 0, \\ B_1 &= \frac{1}{3}\left[1 + \exp\left(\frac{-\mathrm{i}\pi}{3} - \mathrm{i}\theta_1\right)\right], B_2 = 0, B_3 = -\tfrac{1}{6} + \mathrm{i}K, \end{aligned} \tag{A 8}$$

where K is an arbitrary constant and $\theta_1 = \theta_q$ for $q_1 = \pi/(3a)$.

We obtain the following expressions:

$$\begin{aligned} U_n &= \left[\frac{4}{3}\cos\left(n\frac{\pi}{3}\right) - \frac{1}{3}(-1)^n\right], \\ V_n &= \left[-\frac{4}{3}\cos\left(n\frac{\pi}{3} + \frac{2\pi}{3}\right) + \frac{1}{3}(-1)^n\right]. \end{aligned} \tag{A 9}$$

The schema of displacements proposed is composed of one acoustic phonon with $q_1 = \pi/(3a)$ and two optical phonons with $q_1 = \pi/(3a)$ and $q_3 = \pi/a$.

References

Avrami, M., 1939 *J. chem. Phys.*, **7**, 1103.

Burgers, W. G., 1934, *Physica*, **1**, 561.

Dammak, H., Barbu, A., Dunlop, A., Lesueur, D., and Lorenzelli, N., 1993, *Phil. Mag. Lett.*, **67**, 253.

Dammak, H., Dunlop, A., and Lesueur, D., 1996, *Nucl. Instrum. Meth.* B, **107**, 204.

Dobromyslov, A. V., and Taluts, N. I., 1990, *Phys. Metals Metallogr.* (USSR), **69**, 98.

Dobromyslov, A. V., Taluts, N. I., Demchuk, K. M., and Martem'yov, A. N., 1988, *Phys. Metals Metallogr. (USSR)*, **65**, 156.

Dunlop, A., Lesueur, D., Jaskierowicz, G., and Schildknecht, J., 1989, *Nucl. Instrum. Meth.* B, **36**, 412.

Jyoti, G., Joshi, K. D., Gupta Satish, C., Sikka, S. K., Dey, G. K., and Banerjee, S., 1997, *Phil. Mag. Lett.*, **75**, 291.

LANDAUER, R., 1952, *J. appl. Phys.*, **23**, 779.
LEGRAND, B., 1984, *Phil. Mag.* B, **49**, 171.
LESUEUR, D., and DUNLOP, A., 1993, *Radiat. Effects Defects Solids*, **126**, 163.
RABINKIN, A., TALIANKER, M., and BOTSTEIN, O., 1981, *Acta metall.*, **29**, 691.
SASS, S. L., 1972, *J. less-common Metals*, **28**, 157.
SIKKA, S. K., VOHRA, Y. K., and CHIDAMBARAM, R., 1982, *Prog. Mater. Sci.*, **27**, 245.
SILCOCK, J. M., 1958, *Acta metall.*, **6**, 481.
SINGH, A. A., MURALI, M., and DIVAKAR, C., 1983, *J. appl. Phys.*, **54**, 5721.
SONG, G., and GRAY, G. T., 1995, *Phils. Mag.* A, **71**, 275.
STASSIS, C., ARCH, D., and HARMON, B. N., 1979, *Phys. Rev.* B, **19**, 181.
TYSON, W., 1967, *Acta metal.*, **15**, 574.
USIKOV, M. P., and ZILBERSHTEIN, V. A., 1973, *Phys. Stat. sol.* (a), **19**, 53.
VOHRA, Y. K., SIKKA, S. K., MENON, E. S. K., and KRISHNAN, R., 1980, *Acta metall.*, **28**, 683.
ZILBERSHTEIN, V. A., NOSOVA, G. I., and ESTRIN, E. I., 1973, *Fiz. Metall. Metalloved.*, **35**, 584.